

# Remotely-doped superlattices in wide parabolic GaAs/Al<sub>x</sub>Ga<sub>1-x</sub>As quantum wells

J. H. Baskey, A. J. Rimberg, Scott Yang, and R. M. Westervelt  
*Division of Applied Sciences and Department of Physics, Harvard University,  
Cambridge, Massachusetts 02138*

P. F. Hopkins and A. C. Gossard  
*Department of Electrical and Computer Engineering and Materials Department,  
University of California, Santa Barbara, California 93106*

(Received 27 April 1992; accepted for publication 24 July 1992)

Using the digital alloy technique, a series of high-mobility remotely doped GaAs/AlGaAs coupled multiple quantum well structures have been produced by the superposition of a wide parabolic quantum well and a square superlattice potential. Structures containing up to twenty superlattice periods with low temperature Hall mobilities from 23 000 to 100 000 cm<sup>2</sup>/V s have been produced. Fourier analysis of low field Shubnikov-de Haas oscillations, capacitance-voltage and Hall measurements of a 200 Å period superlattice in a 1600 Å wide parabolic well indicate the occupation of four superlattice periods with subband spacings in good agreement with theory.

Semiconductor superlattices have been studied for many years for their interesting physical properties and applications.<sup>1,2</sup> The electron mobility in these structures at low temperatures is typically limited by ionized impurity scattering.<sup>3</sup> A large improvement in mobility was achieved by modulation doping in which the donors are placed in the superlattice barriers.<sup>4</sup> Considerably larger mobilities have recently been achieved by removing the dopant atoms from the superlattice altogether using a wide parabolic well (WPBW) superimposed with a superlattice, as shown in Fig. 1(a). The finite width of the parabolic potential restricts the number of superlattice periods forming the coupled multiple quantum well structure. Parabolic structures with both sinusoidal<sup>5</sup> and square<sup>6</sup> superlattices were recently reported. In this letter we present a quantitative comparison of Shubnikov-de Haas oscillation data with theory and capacitance-voltage profiles, which demonstrate high quality remotely doped square superlattices.

In WPBWs, the parabolically varying band edge, by Poisson's equation, mimics a uniform positive charge distribution of three dimensional density  $n_{3D} = 8\epsilon\Delta/e^2w^2$ , where  $w$  and  $\Delta$  are the width and height of the parabolic potential,  $\epsilon$  is the dielectric constant, and  $e$  is the electronic charge. The electrons from dopants placed outside the parabola move to screen this fictitious charge forming a uniform electron gas of width  $w_e = n_s/n_{3D}$  and sheet density  $n_s$  inside the parabolic well.<sup>7,8</sup> When a superlattice of sufficiently short period is superimposed on the parabolic background, the electrons can screen the parabolic potential but not that of the superlattice,<sup>9</sup> producing a self-consistent potential as shown in Fig. 1(b): the electron density is spatially modulated by the superlattice potential, but the average electron density is approximately  $n_{3D}$ .

The samples were grown via molecular beam epitaxy (MBE) using the digital alloy technique.<sup>7</sup> The average Al concentration along the growth direction was varied by computer-controlled shuttering of the Al furnace, allowing control of the band edge profile during growth of the WPBW with superlattice. Before well growth, the Al con-

centration versus position in the well was measured with an ion gauge substituted for a wafer in the MBE chamber. This information was used to correct for the shutter response time, improving control of barrier width and height, and minimizing deviations from parabolicity.

In this letter we discuss one sample SL6, with 83 meV high, 80 Å wide superlattice barriers inside a parabolic well of width  $w=1600$  Å and height  $\Delta=210$  meV. These parameters were chosen so that the Fermi level lies in the gap between the first and second minibands of the superlattice potential. Carriers were supplied by Si dopants set back 105 Å from the well edges, in delta-doped sheets on either side of the well in a fine AlAs/GaAs superlattice with a period 21 Å and average Al concentration  $x=0.35$ . From the depth of the donors below the conduction band edge<sup>10</sup> the well was expected to be only partially full at liquid He temperatures. This well was one of a series of superlattice structures also investigated. Samples containing 8–20 periods with a range of characteristics were grown and tested. For all, the bandwidth of the lowest miniband was maintained at 2 meV and the superlattice period was fixed at  $d=200$  Å. Barrier widths  $b$  ranged from 40 to 80 Å and barrier heights  $h$  from 83 to 175 meV. The parabolic well width  $w$  ranged from 1600 to 4000 Å and height  $\Delta$  from 87.5 to 210 meV (see Fig. 1), corresponding to a range of electron density from  $n_{3D}=4.0\times 10^{15}$  to  $4.6\times 10^{16}$  cm<sup>-3</sup>.

The sample was cooled in the dark inside a top-loading

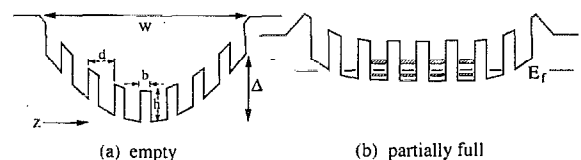


FIG. 1. Schematic diagram of (a) an empty and (b) a partially full wide parabolic well with superlattice. The Fermi level for the partially full well is indicated to lie between the two lowest energy bands represented by the hatched regions.

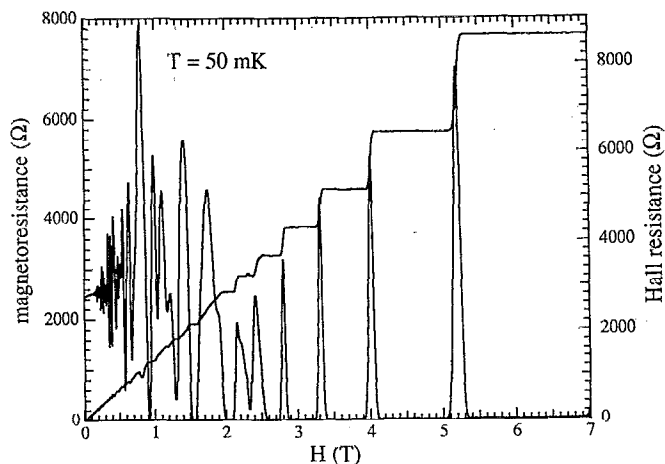


FIG. 2. Magnetoresistance and Hall effect data for sample SL6.

Oxford Model 200 dilution refrigerator. Using standard low frequency lock-in techniques, magnetotransport measurements were made at  $T=50$  mK. Low currents (less than 1 nA) and slow magnetic field sweeps (less than 0.04 T/min) were used to avoid sample heating. The magnetoresistance and Hall effect data are shown in Fig. 2 from which a Hall sheet density of  $n_s=4.3 \times 10^{11} \text{ cm}^{-2}$  and mobility  $\mu=23\,000 \text{ cm}^2/\text{V s}$  were obtained. This mobility is several times greater than that achieved in standard modulation doped superlattices which typically have mobilities less than  $10\,000 \text{ cm}^2/\text{V s}$ .<sup>2</sup> The integer quantum Hall effect is observed with the location of the magnetoresistance zeros consistent with the low field Hall sheet density. Hall steps up to  $\nu=20$  can be identified in the data. In strong magnetic fields above 3 T, a simple estimate predicts that only the lowest Landau level of the lowest miniband states is occupied. In weaker magnetic fields below 3 T, higher Landau levels are also occupied and a complex series of level crossings occurs, resulting in missing or weak Hall plateaus as shown in Fig. 2. Characteristic missing quantum Hall steps also occur in wide parabolic wells without superlattices in which several subbands are occupied.<sup>11</sup>

Multiply periodic Shubnikov-de Haas (SdH) oscillations in the magnetoresistance data were used to measure the Fermi level and subband energies of the superlattice sample. The magnetoresistance oscillation associated with a given occupied subband is periodic in inverse magnetic field  $1/H$  with period  $\hbar e/m_e(E_f - E_i)$ , where  $m_e=0.067 m_0$  is the electron effective mass,  $E_i$  is the bottom of the  $i$ th subband, and  $E_f$  is the Fermi energy, both in zero field. We assume that the two spin states of each subband are not

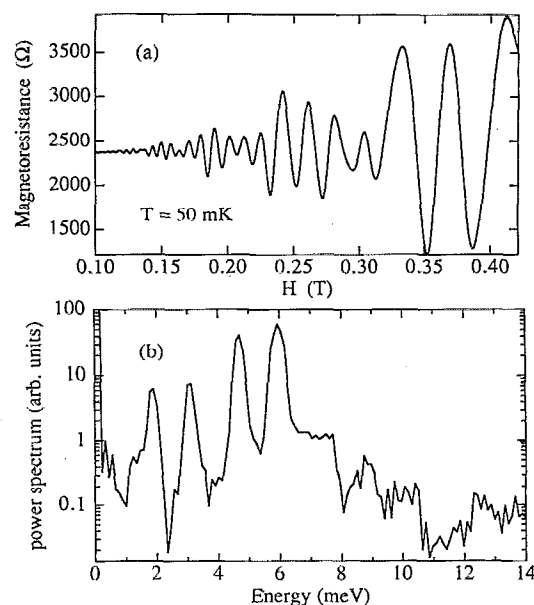


FIG. 3. (a) Multiply periodic low field SdH oscillations for sample SL6 indicating the occupation of several subbands and (b) the power spectrum of the SdH oscillations over the field range  $H=0.03\text{--}0.35$  T.

resolved at the low magnetic fields used for this measurement. Using this expression, the separations  $(E_f - E_i)$  between the Fermi level and the subband bottoms can be calculated by Fourier analysis of the SdH oscillations, and the total sheet density  $n_s$  can be determined by summing the contributions from each subband  $n_s = \sum m_e(E_f - E_i) / \pi \hbar^2$ . Magnetoresistance data for magnetic fields less than 0.4 T at  $T=50$  mK are shown in Fig. 3(a) together with the corresponding SdH power spectrum in Fig. 3(b) computed from interpolated magnetoresistance data spaced equally in  $1/H$ . For convenience, the horizontal axis of the power spectrum in Fig. 3(b) has been given in electron energy  $(E_f - E_i)$  using the expression for the SdH period given above. Four peaks are clearly visible in the power spectrum, indicating that four subbands of the superlattice are occupied, each with two spin states. The total sheet density obtained by summing subbands is  $n_s=4.4 \times 10^{11} \text{ cm}^{-2}$ , in excellent agreement with the Hall sheet density  $n_s=4.3 \times 10^{11} \text{ cm}^{-2}$ . Table I lists the measured Fermi level  $E_f$  and the energies  $E_i$  of the occupied subbands, all given relative to the lowest subband  $E_1$ .

To compare these experimental results with theory, a self-consistent solution of Schrödinger's and Poisson's equation, including the exchange-correlation potential in

TABLE I. Comparison of Shubnikov-de Haas measurements of the Fermi energy and subband energies with theory; all energies are in meV.

	Experiment	Theory-Superlattice		Theory-Parabola	
		(1370 Å)	(1370 Å)	(1370 Å)	(1600 Å)
$E_f - E_1$	$5.93 \pm 0.06$	5.89	7.98	6.56	
$E_2 - E_1$	$1.22 \pm 0.10$	1.23	2.34	1.36	
$E_3 - E_1$	$2.79 \pm 0.14$	2.78	5.71	3.43	
$E_4 - E_1$	$4.03 \pm 0.14$	4.17	...	6.10	

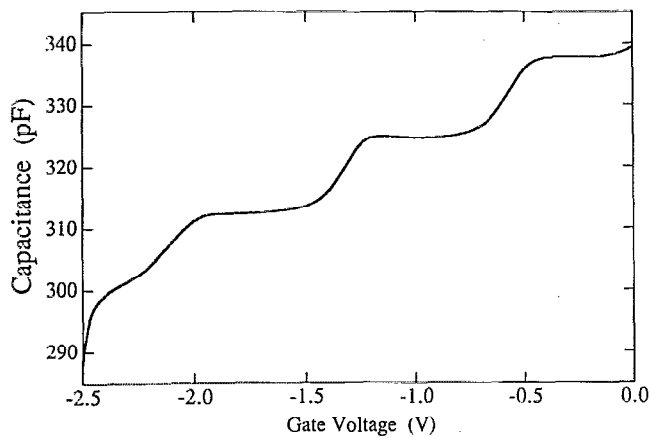


FIG. 4. Capacitance vs gate voltage at  $T=0.43$  K. Each step corresponds to an occupied period of the superlattice system. As the electron layer in the period nearest the gate is depleted the capacitance shifts to the value associated with the occupied period next nearest the gate.

the local density functional approximation,<sup>12</sup> was calculated using the experimentally determined sheet density as input, assuming symmetric filling about the well center. The parabolic well width is position dependent because the source guns are angled with respect to the wafer, and the wafer is not rotated during growth to avoid aliasing effects, resulting in a uniform gradation in well width across the sample. A 20% gradient in the growth rate of GaAs across unrotated test wafers was measured via RHEED oscillations. Using the parabolic well width as the only adjustable parameter we found excellent agreement, shown in Table I, between experiment and theory for a well which is 1370 Å wide, well within the range of growth parameters. Table I also shows theoretical energy level spacings for WPBWs identical to SL6 with widths 1370 and 1600 Å but no superlattice. It is clear the measured energy levels are not those of a plain WPBW; the level of agreement cannot be significantly improved by altering the well width. The spacing of the observed subband energies is relatively uniform, and the Fermi energy is reduced relative to a simple WPBW, as expected for a superlattice.<sup>9</sup>

The electron density profile in the superlattice was directly probed using capacitance-voltage measurements.<sup>13</sup> The sample was cooled in the dark to 0.43 K in a pumped He-3 immersion system. The capacitance between a Cr/Au front gate evaporated on the sample and the electron gas in the parabolic well was measured using lock-in techniques with a superimposed ac voltage (20 mV<sub>rms</sub>@402 Hz) and dc voltage applied between the gate and the electron gas as the width of the gas was swept to depletion. Experimental results were checked for several different frequencies and amplitudes of the applied ac signal with good agreement. The measured  $C$ - $V$  profile shown in Fig. 4 has four well-defined plateaus, indicating that the electron density profile has four well-defined layers in agreement with the calculated number of occupied superlattice wells for the measured sheet density and parabolic well width  $w=1370$  Å. From the steps in capacitance between plateaus in Fig. 4, we determined that the electron layers were uniformly

spaced at  $175 \pm 10$  Å consistent with the spacing obtained from SdH data above.

Combining the number of occupied superlattice periods from  $C$ - $V$  data with the number of occupied subbands from SdH data, we find that one subband with two spin states is occupied for each of four superlattice periods. It is interesting to interpret these results in terms of a simple tight-binding model. In the absence of electrons, the individual square wells of the superlattice are not aligned in energy as they are superimposed on a parabolic potential. In a full well the parabolic potential is approximately cancelled by the electrostatic potential of the electron layer, bringing all superlattice wells into energy alignment. For the sample studied here the WPBW is half full so only four superlattice periods are occupied and in approximate energy alignment. The lowest miniband of a tight binding model for this case is full, with four energy levels and two spin states per level. This configuration is consistent with the design of the structure, for which the Fermi energy lies in the gap above the lowest miniband (see Fig. 1).

In summary we have produced and characterized remotely doped high-mobility multiple quantum well structures with a range of three-dimensional electron densities from  $n_{3D}=4.0 \times 10^{15}$  to  $4.6 \times 10^{16}$  cm<sup>-3</sup>. Magnetotransport and  $C$ - $V$  measurements for one structure show a spatially modulated electron density profile occupying four periods of a square superlattice potential, demonstrating control of both the electron density profile and energy subband structure of a wide electron gas.

We thank Jed Dempsey for valuable comments. One of the authors (J.H.B.) acknowledges support from the Natural Science and Engineering Research Council of Canada. Work at Harvard was supported in part by the National Science Foundation and by the Harvard Materials Research Laboratory under Grants DMR-91-19386 and DMR-89-20490; work at Santa Barbara was supported by the Air Force Office of Scientific Research under Grant AFOSR-91-021.

<sup>1</sup>L. Esaki and R. Tsu, IBM J. Res. Dev. **14**, 61 (1970).

<sup>2</sup>H. L. Störmer, J. P. Eisenstein, A. C. Gossard, W. Wiegmann, and K. Baldwin, Phys. Rev. Lett. **56**, 85 (1986).

<sup>3</sup>See, for example, K. Seeger, *Semiconductor Physics* (Springer, New York, 1973), p. 170.

<sup>4</sup>R. Dingle, H. Stormer, A. C. Gossard, and W. Wiegmann, Appl. Phys. Lett. **33**, 665 (1978).

<sup>5</sup>J. Jo, M. Santos, M. Shayegan, Y. W. Suen, L. W. Engel, and A. M. Lanzilotto, Appl. Phys. Lett. **57**, 2130 (1990).

<sup>6</sup>A preliminary report of this work appears in Proc. NanoMES'91, Santa Fe, New Mexico, Superlatt. Microstruct. **11**, 317 (1992).

<sup>7</sup>M. Sundaram, A. C. Gossard, J. H. English, and R. M. Westervelt, Superlatt. Microstruct. **4**, 683 (1988).

<sup>8</sup>M. Shayegan, T. Sojoto, M. Santos, and C. Silvestre, Appl. Phys. Lett. **53**, 791 (1988).

<sup>9</sup>L. Brey, N. F. Johnson, and J. Dempsey, Phys. Rev. B **42**, 2886 (1990).

<sup>10</sup>N. Chand, T. Henderson, J. Klem, W. T. Masselink, R. Fischer, Y. Chang, and H. Morkoç, Phys. Rev. B **30**, 4481 (1984).

<sup>11</sup>E. G. Gwinn, R. M. Westervelt, P. F. Hopkins, A. J. Rimberg, M. Sundaram, and A. C. Gossard, Phys. Rev. B **39**, 6260 (1989); K. Ensslin, M. Sundaram, A. Wixforth, J. H. English, and A. C. Gossard, Phys. Rev. B **43**, 9988 (1991).

<sup>12</sup>A. J. Rimberg and R. M. Westervelt, Phys. Rev. B **40**, 3970 (1989).

<sup>13</sup>M. Sundaram, A. Wixforth, P. F. Hopkins, and A. C. Gossard, J. Appl. Phys. (to be published).